UNIVERSITY *of the* WESTERN CAPE

Poisoning-tolerant metal hydride materials and their application for hydrogen separation from CO_2/CO containing gas mixtures

K.D. Modibane, M. Williams, M. Lototskyy, M.W. Davids, Ye. Klochko and B.G. Pollet

Abstract
Metal hydride materials offer attractive solutions in addressing problems associated with hydrogen separation and purification from waste flue gases. However, a challenging problem is the deterioration of hydrogen charging performances resulting from the surface chemical action of electrophilic gases. In this work, the feasibility study of poisoning tolerance of surface modified AB_5-type hydride forming materials and their application for hydrogen separation from process gases containing carbon dioxide and monoxide was carried out. Target composition of $La(Ni,Co,Mn,Al)_5$ substrate was chosen to provide maximum reversible hydrogen capacity at the process conditions. The selected substrate alloy has been shown to be effectively surface-modified by fluorination followed by electroless deposition of palladium. The surface-modified material exhibited good coating quality, high cycle stability and minimal deterioration of kinetics of selective hydrogen absorption at room temperature, from gas mixtures containing 10% CO_2 and up to 100 ppm CO. The experimental prototype of a hydrogen separation unit, based on the surface-modified metal hydride material, was tested and exhibited stable hydrogen separation and purification performances when exposed to feedstocks containing concentrations of CO_2

1. Introduction

Metal hydride (MH) materials have found a number of promising gas-phase applications in processes of considerable economic potential, such as hydrogen storage, separation and recovery, thermally-driven compressors and heat pumps, etc. [1e3]. These materials exhibit a favourable combination of their properties, including reversibility and selectivity of interaction with H_2 gas at mild conditions, high volumetric density of hydrogen in the solid, significant heat effects in the course of hydrogenation/dehydrogenation. Thus they are very flexible in the applications, and often allow to develop multifunctional facilities (e.g., for hydrogen storage, purification and controlled supply) which offer to an end-user safe, efficient and cost-saving solutions [4].

A number of process developments utilising MH for separation and purification of hydrogen were undertaken since 1970th [5e15]. Mainly, the solutions [8,9,13,14], use AB_5-type hydrogen storage intermetallides to extract H_2 from process gases typical for production of ammonia (N_2, Ar, hydrocarbons and NH_3 impurities; up to 50% in total); the process conditions cover temperature range from 20 to 150 ^{O} C and pressures 10e100 bar H_2. Some of these developments were implemented on industrial-scale [9,14]. Feasibility studies of application of MH for hydrogen extraction from gas mixtures containing CO_2 and CO were also reported, and the suitable solutions were suggested [5,7,16,17].

The H absorption process often requires higher temperatures and, correspondingly, usage of hydride-forming materials characterised by higher hydride stabilities: $LaNi_4Cu$ [5], Ti-based alloys and composites [7,16], activated Mg [12], or Pd alloy [15]. At the same time, a challenging problem that hampers application of MH for hydrogen separation from the mixtures containing chemically-aggressive gases (O_2, H_2O, CO, sulphur-containing compounds, etc.) is the deterioration of MH performances as a result of the presence in hydrogen of gas impurities [3,18] able to easily react with MH surfaces resulting in the formation of surface compounds (oxides and hydroxides, carbonyls, sulphides) which seriously limit hydrogen absorption. Most probably, the impurities deactivate surface centres responsible for H_2 dissociation (e.g., Ni clusters for AB_5-type alloys) resulting in the retardation of this process, which represents the rate-limiting step in hydrogen absorption [19,20].

So far, two approaches were implemented to address the above-mentioned problem. The first one includes removal of the impurities prior to H absorption in the MH [17] while the second improves the poisoning tolerance of MH by their surface modification [20e23].

In our previous studies [24e28] we investigated the influence of surface modification (by fluorination and/or electroless deposition of metals, including Pd) of AB_5-type alloys on their activation performances and poisoning tolerance. The corresponding surface modification procedures for the preparation of the advanced materials were developed [29,30], and feasibility of their application for hydrogen purification from (CO_2 þ CO)-containing gases was demonstrated [31,32]. The novel features of the developed surface modification procedures include (i) enhancement of PGM deposition by surface functionalisation of the metallic hydride-forming material [25,28,29], and (ii) combination of fluorination and enhanced PGM deposition procedures [24,28,30].

This investigation presents further feasibility study of hydrogen absorption from mixed gas feedstocks, by unmodified and surface-modified (using the fluorination

2

e Pd encapsulation technique) La(Ni,Mn,Al,Co)$_5$ alloy, which was subsequently utilised for testing of a prototype hydrogen extraction and purification system.

2.   Experimental

The AB$_5$-type substrates were initially arc-melted at the Institute for Energy Technology (IFE) using high-purity starting materials, annealed for 72 h at 1000 $^{\mathrm{O}}$C in vacuum, and crushed in a mortar. Quantities of the AB$_5$ materials for prototyping applications were purchased from Guangzhou Research Institute of Non-Ferrous Metals.

Surface modification of the substrate material was conducted through fluorination and followed by autocatalytic deposition of Pd at the South African Institute for Advanced Materials Chemistry (SAIAMC). The rationale behind this approach was the combination of the large increase in the specific surface area of the material with fluorination, and the enhanced activation kinetics observed with deposition of Pd catalytic layers, to form materials with exquisite hydrogen sorption properties. The fluorination and autocatalytic deposition of Pd were applied to w300 g batch of the La(Ni,Co,Al,Mn)$_5$ substrate. Further details on the surface modification procedure and characterisation (including activation performances) of the surface-modified materials can be found elsewhere [21,24,28,30,32].

The hydrogen absorption/desorption performances (PCT diagrams) of several substrate alloys were measured using a PCT Pro-2000 gas sorption analyzer (Hy-Energy LLC) at T = 50-200 $^{\mathrm{O}}$C and P$_{H2}$ = 0-50 bar H$_2$. The raw PCT data were pre-processed using macros HyDataAnalysis Version 2.2.3, © Hy-Energy 2007 supplied as auxiliary software together with the instrument, in the environment IgorPro Version 6.0.3.1, © WaveMetrics Inc. The pre-processing, in particular, introduced correction into the calculation of amount of absorbed/ desorbed hydrogen taking into account displacement volume. Further PCT data processing was done using the model of phase equilibria in metalehydrogen systems reported by Lototskyy et al. [33]. The absorption and desorption datasets were processed separately.

Kinetics of hydrogen absorption from pure H$_2$ and gas mixtures by MH material, in a running flow mode, was studied using procedures similar to one reported earlier [28,31]. The MH material (m w 4 g) was loaded in the running-flow tubular reactor (internal diameter e 10 mm). Activation of the MH sample and determination of amount of hydrogen absorbed from the feeding gas for the specified period of time was carried out using a Sieverts-type installation. The experiments were carried out as follows: after activation (3 cycles of 1-h vacuum heating to 200 $^{\mathrm{O}}$C followed by absorption of pure H$_2$ at room temperature), the sample was evacuated at 200 $^{\mathrm{O}}$

C for 1 h and cooled to the operational temperature (20 ^{o} C). The sample was exposed to the flow of the feeding gas at the constant flow rate (0.25 and 1 L/min STP for pure H_2 and gas mixture containing 25% H_2, respectively) and pressure (2.0 bar for pure H_2, 8.0 bar for the mixture), for the specified period (1e30 min). Hydrogen absorption rates, r, in the running-flow mode were estimated using simplified thermal calculations according to the formula[1]:

$$r = C_H \frac{\Delta T}{\int_0^{\tau_{MAX}} \Delta T d\tau} \qquad (1)$$

where DT is the difference between actual (T) and starting (T$_0$) sample temperature, s is time.
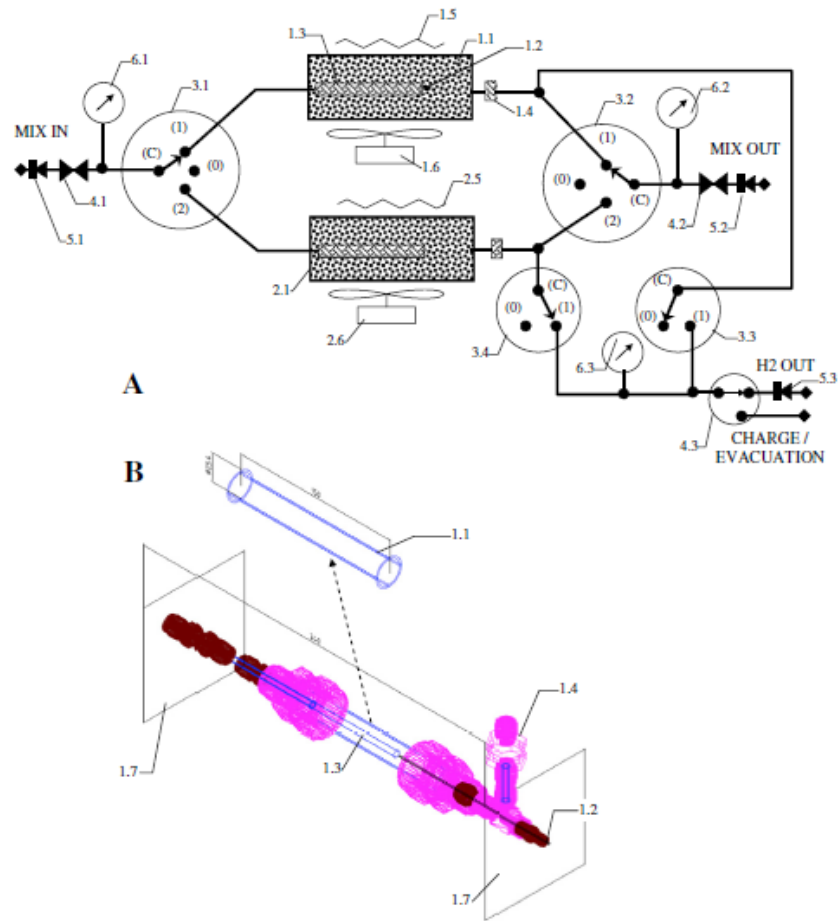
1, 2 – Reactor assemblies:

    1.1 (2.1) – Reactors with MH material:

    1.2 – Thermocouple,

    1.3 – Input gas filter,

    1.4 – Output / inline gas filter,

    1.5 (2.5) – Electric heaters,

    1.6 (2.6) – Air coolers,

    1.7 – Holding plate;

3 – Remote controlled valves:

    3.1 – Input of the feed gas,

    3.2 – Venting of the unreacted feed gas,

    3.3 – Output of pure H_2 from reactor 1,

    3.4 – Output of pure H_2 from reactor 2;

4 – Manually operated valves:

    4.1 – Input of the feed gas,

    4.2 – Venting of the unreacted feed gas,

    4.3 – Output of pure H_2;

5 – One-way (check) valves:

    5.1 – Input of the feed gas,

    5.2 – Venting of the unreacted feed gas,

    5.3 – Output of pure H_2;

6 – Pressure gages:

    6.1 – Input of the feed gas,

    6.2 – Venting of the unreacted feed gas,

    6.3 – Output of pure H_2.

Fig. 1 – Schematics of the experimental MH system for H2 extraction (A) and layout of the reactor assembly (B).

5

Hydrogen concentration, C_H, and rates of hydrogen desorption from the hydrogenated sample were determined volumetrically, using preliminary evacuated Sieverts-type installation connected to the reactor, when the sample was heated from 20 to 200 ^{O}C, heating rate w5 deg/min.

Testing of the material for hydrogen separation and purification was studied using a hydrogen extraction and purification system (Fig. 1). The system included two running-flow reactor assemblies (1, 2), each reactor contained 140 g of the surface-modified MH material and equipped with electric heaters (1.5, 2.5) and air coolers (1.6, 2.6) whose operation was synchronised with switching gas flows by motorised valves (3). The reactors were working in the opposite phases, i.e. H_2 absorption from the feeding gas in a cooled reactor with the simultaneous desorption of pure H_2 from the heated one. The reactor (Fig. 1(B)) was built on the basis of standard stainless steel tube (1.1), 1^{OO} (25.4 mm) in diameter, 0.083^{OO} (2.11 mm) in wall thickness. The internal space of the reactor, in between the body tube (1.1) and coaxially placed $1/4^{OO}$ OD gas supply tube assembled with a tubular filter (1.3; 0.5 m in pore size), was filled with the powder of $LaNi_{3.55}Mn_{0.4}Al_{0.3}Co_{0.75}$ surface-modified by fluorination and autocatalytic deposition of Pd (300 g batches of the alloy powder). The filling density of the MH in the reactor was about 50% of the density of the material in the hydrogenated state. The reactor was assembled using standard Swagelok$^{®}$ tube fittings allowing for operation at temperatures up to 500 ^{O}C and gas pressures up to 200 bar.

The system was installed on a testing workbench providing all the operation modes, including supply of feed gas with parallel output of the extracted and purified hydrogen, and activation/regeneration of the MH material (evacuation and supply of pure hydrogen).

The workbench also provided mass spectrometric analysis of the gas supplied from one selected point of three: input of the feeding gas, venting of the feeding gas, and output of pure hydrogen. The composition of the gas was analysed using a QMS200 mass spectrometer (Stanford Research Systems, USA) equipped with O100SSC capillary. The analysis was conducted by continuous scanning in the mass number range m/z = 1-50 a.m.u., with the resolution of 10 points/a.m.u., using electron impact ionisation (70 eV). The presented mass spectra corresponded to the average of 6e12 scans taken in the middle of the 15 min-long absorption/desorption cycle, at sampling pressure 0.2-0.3 bar. The latter value corresponds to the total gas pressure in the ion source about 1.10^{-5} Torr. The sensitivity of the instrument at these conditions was about 1.10^{-10} Torr roughly corresponding to detectable concentration about 10 ppm (1 ppm for H_2). The instrument was calibrated by the recording reference mass spectra taken at the same ionisation conditions for individual gases (Ar, CO_2, N_2, CO, O_2, CH_4,

6

H$_2$; Afrox Ltd., purity > 99.99%) at the sampling pressure 1 bar (~3.10^{-5} Torr in the ion source). The calibration data presented in Supplementary information (Table S1) also include estimated intensities of peaks m/z = 17, 18 for water vapours at the same sampling pressure.

During the tests, the cycle duration was set within 10-30 min; lower (H absorption, T$_L$) and higher (H desorption, T$_H$) temperatures were set as T$_L$ = 20-100 ^{O}C, T$_H$ = 150-200 ^{O}C; feed gas was supplied at flow rate of 1-5 L/min and the pressure 5e15 bar; H$_2$ output was carried out at P = 1-1.5 bar. The rate of selective hydrogen absorption in the cooled reactor was calculated starting from the difference of readings of flow controller and flow meter installed in the gas mixture supply and venting lines, respectively. The flow rate of output hydrogen was measured directly, by a flow meter installed in the H$_2$ output line.

Further details on the prototype H$_2$ separation system, its operation and testing can be found elsewhere [31,32].

The experiments were carried out using gas mixtures 25% H$_2$ + 0-30% CO$_2$ + 0-100 ppm CO + N$_2$ (balance) as a feed gas. The mixtures were supplied by Air Liquide South Africa. Precise compositions of the mixtures used for the tests of the hydrogen separation system (the analysis was carried out by the supplier) are presented in Table 1.

3.   Results and discussion

Selection of the substrate material was based on the requirement to provide maximum reversible hydrogen capacity at the operation conditions typical for processing of a carbonaceous feedstock including desulphurization, steam reforming and water-gas shift. It assumes H$_2$ absorption at its partial pressure up to 2.5 bar (T ≤ 80 ^{O}C) followed by H$_2$ desorption at T = 200 ^{O}C and P ≥ 1 bar.

Table 2 summarises the PCT data presented as hydrogen sorption capacities of the studied AB$_5$-type substrate alloys at the conditions specified above. The corresponding values were obtained by the fitting of the experimental data by the model [33]. An example for LaNi$_{3.55}$Co$_{0.75}$Mn$_{0.3}$Al$_{0.4}$ is shown in Fig. 2 as a 3D PCT plot (a); and calculated absorption and desorption isotherms (b) for the temperatures of 80 and 200 ^{O}C, respectively.

It can be seen from Table 2 that at the applied experimental conditions the highest reversible hydrogen sorption capacity among the studied AB$_5$-type alloys was exhibited by LaNi$_{3.55}$-Co$_{0.75}$Mn$_{0.3}$Al$_{0.4}$. 2'.80% hydrogenation of this substrate can be reached at hydrogen pressures above 2e2.5 bar and temperatures below 80 ^{O}

C; the dehydrogenation corresponding to the residual hydrogen content in the sample ≤10% of the maximum H capacity takes place at T~200 ^{O}C and $P_{H_2} \leq 1$ bar (Fig. 2(b)). This substrate alloy was selected for further experiments on surface modification and hydrogen separation/ purification.

It was found that $LaNi_{3.55}Co_{0.75}Mn_{0.3}Al_{0.4}$ can be efficiently surface-modified, to yield dense coatings of deposited Pd particles (w200 nm in the size), as shown in Fig. 3(b). Good coating morphology and activation performances of the surface-modified material remained after the application of the surface modification procedure in the upscaled amounts, up to 1.5 kg of the substrate per a load [32]. Depending on the batch size, the surface-modified materials contained 0.7 to 7.9 wt% F and 1.3 to 5.2 wt. Pd (EDS data)[2]; the latter range corresponds to the total Pd loading (AAS) of 0.34e1.35 wt%. The materials also exhibited BET specific surface area (SSA) m^2/g that was significantly higher than the SSA of the unmodified alloy (0.27 m^2/g) but lower than the one for the alloy surface-modified by fluorination without Pd deposition (1.14 m^2/g).

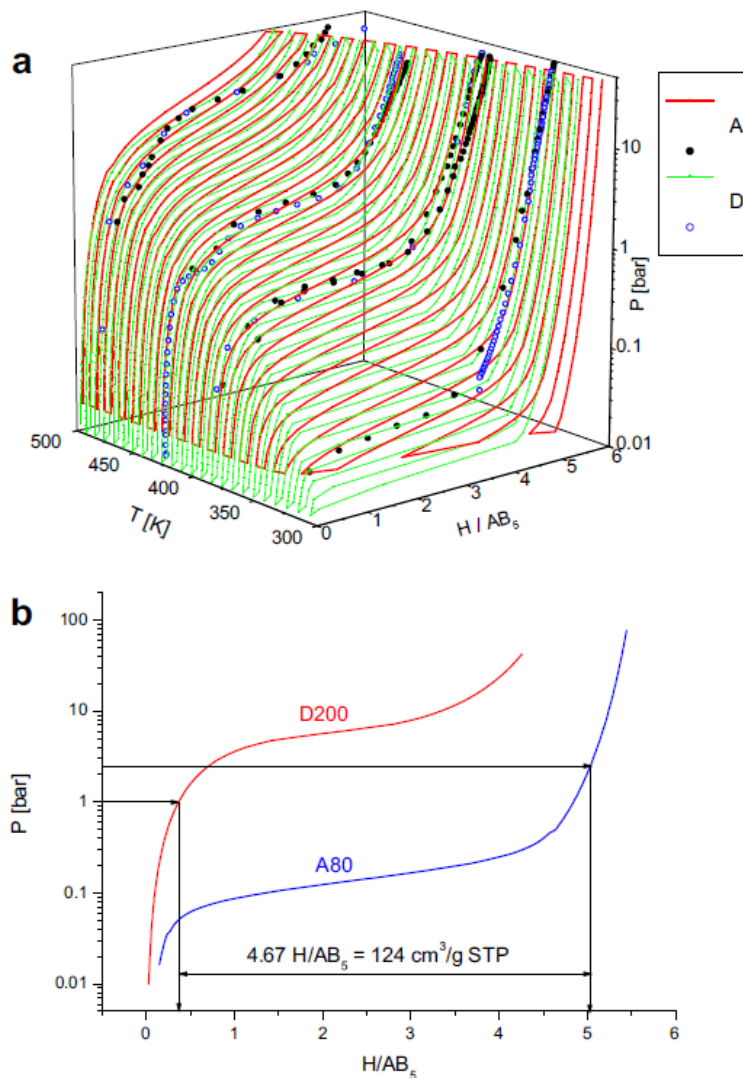| Table 1 — Compositions of gas mixtures according to supplier's certificate.				
Mixture	Components			
	H_2 [%]	CO_2 [%]	CO [ppm]	N_2 [%]
1: 25% H_2 + N_2 (balance)	26.60	–	–	73.40
2: 25% H_2 + 10% CO_2 + 100 ppm CO + N_2 (balance)	25.30	9.70	94.5	65.00
3: 25% H_2 + 20% CO_2 + 100 ppm CO + N_2 (balance)	24.44	19.20	90.6	56.36
4: 25% H_2 + 30% CO_2 + 100 ppm CO + N_2 (balance)	25.50	30.30	92.7	44.20

Fig. 2 – PCT properties of the LaNi$_{3.55}$Co$_{0.75}$Mn$_{0.3}$Al$_{0.4}$ substrate alloy: (a) – 3D PCT plots for absorption (A) and desorption (D), experimental points and calculated trajectories; (b) – calculated isobars of H absorption at $T = 80\ °C$ (A80) and H desorption at $T = 200\ °C$ (D200).

In doing so, the electroless deposition of Pd onto fluorinated AB$_5$ material results in the "plugging" of micro-cavities in the fluoride layer by Pd nanoparticles that, in turn, results in the improvement of hydrogen absorption performances and poisoning tolerance of the surface-odified material [24,28].

The hydrogen absorption rates from pure H$_2$ and gas mixtures containing CO$_2$ and CO, by the unmodified and surface modified La(Ni,Mn,Al,Co)$_5$ are presented in Fig. 4, accompanied by specification of the total quantity of hydrogen (C$_H$) absorbed in the sample during the experimental run. Exposure of the unmodified alloy (Fig. 4(a)) in the gas mixture containing 10% CO$_2$ resulted in immediate deterioration of H$_2$ absorption properties, in agreement with the literature data

9

reporting about strong retardation of hydrogen absorption and decrease of H absorption capacity during cyclic operation of hydride-forming materials at a presence of CO_2 in a feedstock gas [18]. In contrast, the exposure of the surface-modified material (Fig. 4(b)) in the same gas mixture resulted in slight deterioration of the hydrogenation rate and negligible deterioration of the hydrogen absorption performances observed during cyclic operation. Similar observations were previously reported by Wang et al. [21], who observed that the hydrogen charging rate of fluorinated $LaNi_{4.7}Al_{0.3}$ from a CO_2-rich H_2-containing gas mixture is close to that observed from pure hydrogen.

Additional introduction of 100 ppm CO into the feed gas results in significant and fast deterioration of hydrogen absorption capacity of the unmodified alloy (Fig. 4(c)). However, the deterioration of the surface-modified material at these conditions (Fig. 4(d)) remains very small: the material exhibits almost same kinetic performances as in the case of CO_2-containing gas mixture (Fig. 4(b)).

The thermal desorption spectrum (TDS) for the unmodified alloy hydrogenated in pure H_2 (Fig. 5(a) and (c), curve 0) shows that slow hydrogen desorption starts already at room temperature, accelerates at T > 90 ^{0} C, gets a peak at Tw140 ^{0} C and finishes at 195 ^{0} C. The exposure in CO_2- (Fig. 5(a), curves 1, 4) and (CO_2 + CO)-containing (Fig. 5(b), curves 1, 11) gas mixtures during the hydrogenation does not significantly change the TDS behaviour; the decrease of peak height corresponds to the deterioration of H absorption capacity throughout H_2 absorption/desorption cycling. An increase of the peak temperature by 7^{0} was observed for the first H_2 desorption from the material hydrogenated at the presence of CO_2 that could be a result of the alloy surface poisoning. The hydrogenated surface-modified material (Fig. 5(b) and (d)) exhibits lower desorption peak temperatures: 115 ^{0} C after hydrogenation in pure H_2 and 130-135 ^{0} C after H_2 absorption from CO_2- and CO-containing mixtures. The reduction of the peak temperatures is, most probably, caused by catalytic effect of surface Pd which facilitates associative desorption of H_2 molecules.

Table 2 – Hydrogen sorption capacities of the studied AB$_5$-type substrate alloys.

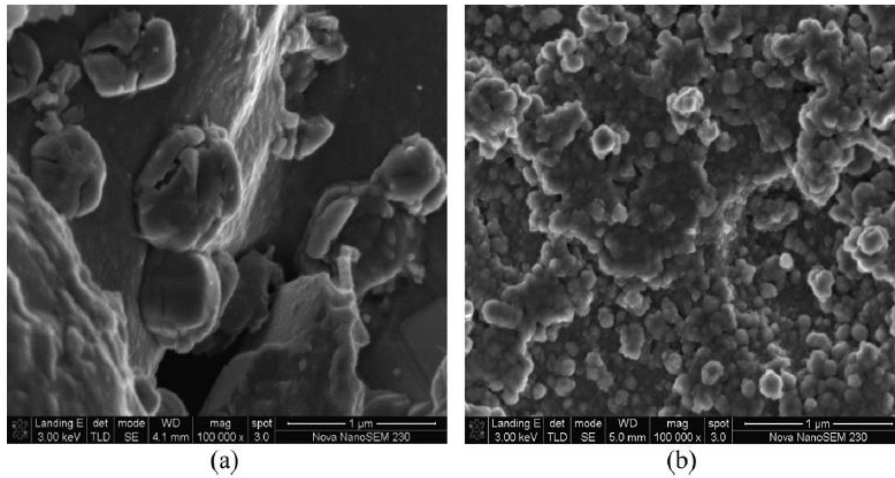| Alloy	Absolute [H/AB$_5$]		Reversible	
	Absorption (80 °C/ 2.5 bar)	Desorption (200 °C/ 1 bar)	[H/ AB$_5$]	[cm^3/g STP]
LaNi$_4$Mn	5.205	1.252	3.953	104
LaNi$_4$Mn$_{0.5}$Co$_{0.3}$Cu$_{0.2}$	3.306	0.092	3.214	85
La$_{0.34}$Ce$_{0.50}$(Pr,Nd)$_{0.16}$ Ni$_{3.15}$Co$_{0.65}$Mn$_{0.6}$Al$_{0.6}$	3.937	0.192	3.745	99
LaNi$_{3.55}$Co$_{0.75}$Mn$_{0.3}$Al$_{0.4}$	5.035	0.368	4.667	124

Fig. 3 – SEM images of (a) unmodified La(Ni,Mn,Al,Co)$_5$ alloy powder and (b) the material after surface modification by fluorination and autocatalytic Pd deposition (NaH$_2$PO$_2$, 30 min).
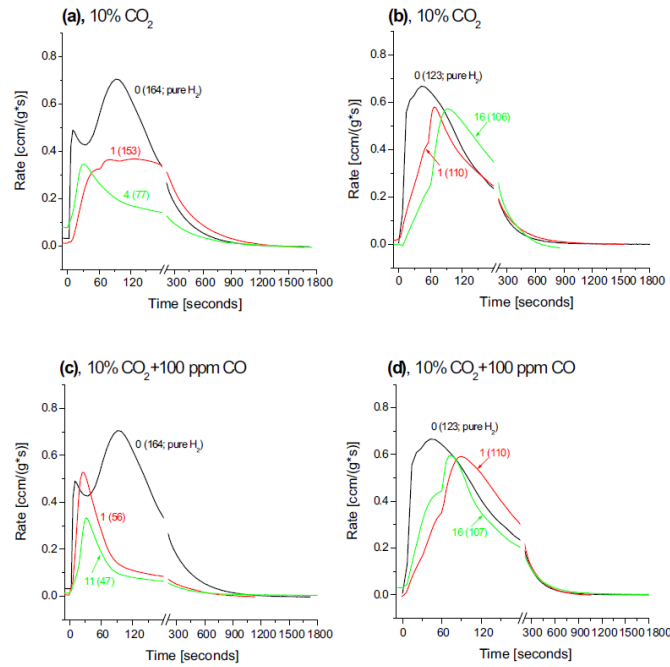
Fig. 4 − Hydrogen absorption rates from gas mixtures by La(Ni,Mn,Al,Co)$_5$ alloy in a running flow mode at $T_0 = 20$ °C. The partial H_2 pressure and flow rate are 2 bar and 0.25 L/min STP, respectively. (a,c) − unmodified alloy; (b,d) − the alloy surface-modified (300 g batch of the substrate) by fluorination and autocatalytic deposition of Pd. Curve labelling: 0 − pure H_2; 1... − mixture H_2 (25%) + CO_2 (+CO) + N_2 (balance). The number corresponds to the number of the absorption cycle. The values in brackets correspond to maximum hydrogen absorption capacity [cm^3/g STP]. Compositions of the feed gas correspond to the presence of 10% CO_2 (a, b) and 10% CO_2 + 100 ppm CO (c, d).
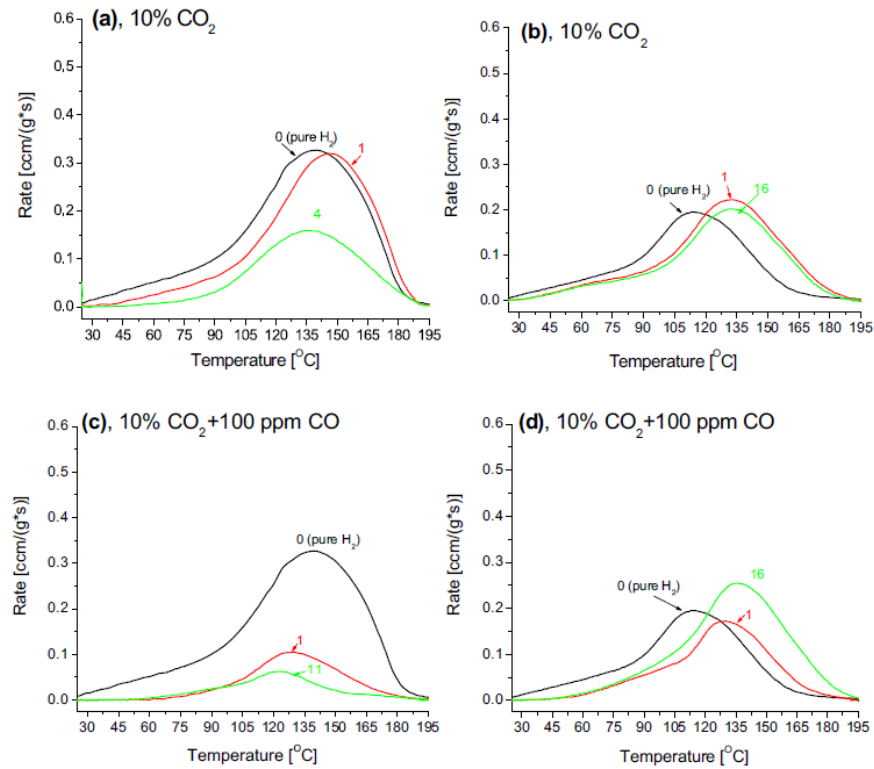

Fig. 5 − Hydrogen thermal desorption spectra from the unmodified (a,c) and surface modified (b,d) La(Ni,Mn,Al,Co)$_5$ material. hydrogenated in the running flow mode. Labelling of the graphs (a−d) and curve numbers correspond to hydrogenation conditions specified in Fig. 4.

12

Fig. 6 shows typical operation cyclograms of hydrogen extraction and purification system. The cyclograms present time dependencies of reactors temperatures (T_1, T_2), as well as flow rates of selective H_2 absorption (FR(IN)) in the cooled reactor and H_2 desorption (FR(OUT)) from the heated one.

The system operation included periodic cooling of one reactor accompanied by hydrogen absorption therein, and simultaneous heating of another reactor accompanied by release of hydrogen. Hydrogen absorption in the cooled MH reactor started immediately after the reactor began to cool down and took place during the whole cooling stage in the studied range of the cycle durations (15-30 min). When the MH temperature decreases to ~80 ^{O} C, the absorption rate reaches a maximum followed by a slow decrease. This effect is more pronounced for higher flow rates of the feed gas (Fig. 6(b)).

The rate of hydrogen desorption from the heated MH reactor under the specified conditions was found to be relatively rapid. The desorption rate reached the maximum (0.7-2.0 L/min STP, depending on the H absorption conditions) in <3 min after initiating heating, and desorption neared completion in ~7 min.

As it can be seen from Fig. 7 summarising the data on hydrogen absorption and desorption capacities of metal hydride reactors during the system operation, introduction of CO_2 and CO in the feed gas does not significantly change the absorption/desorption behaviour, but results in a reduction of the H_2 capacity. The total amount of H_2 absorbed in/desorbed from the reactor within 15 min in all gas mixtures was 3.0-4.0 L (20e27 cm^3/g STP), corresponding to 16-22% of the reversible hydrogen sorption capacity of the substrate alloy under the experimental conditions (Table 2). The increase of feed gas flow rate and cycle time (Fig. 6(b)) results in the increase of the total H_2 amount up to 7.3 L (49 cm^3/g STP), or 40% of the reversible hydrogen capacity of the material. The observed reduction of the H_2 capacity is mainly caused by mass transfer limitations [32]. Further capacity drop at the presence of CO_2 and CO has its origin in the deterioration of H_2 absorption kinetics, very strong for the unmodified material (Fig. 4(c)) but much less pronounced for the surface-modified one (Fig. 4(d)).

Analysis of the presented results confirms our conclusion [32] that the total process productivity of H_2 separation by temperature/pressure swing absorption-desorption in MH reactor is hindered by the slow selective H_2 absorption under the process conditions, limited by mass transfer in the gas phase. This effect is very pronounced even for inert balance gas (N_2), due to the lowering of H_2 partial pressure and, in turn, driving force of the H_2 absorption. Similar results were recently presented in Ref. [34].

Further deterioration of hydrogen separation productivity because of poisoning of MH material by active impurities (CO_2 and CO) was much less pronounced.
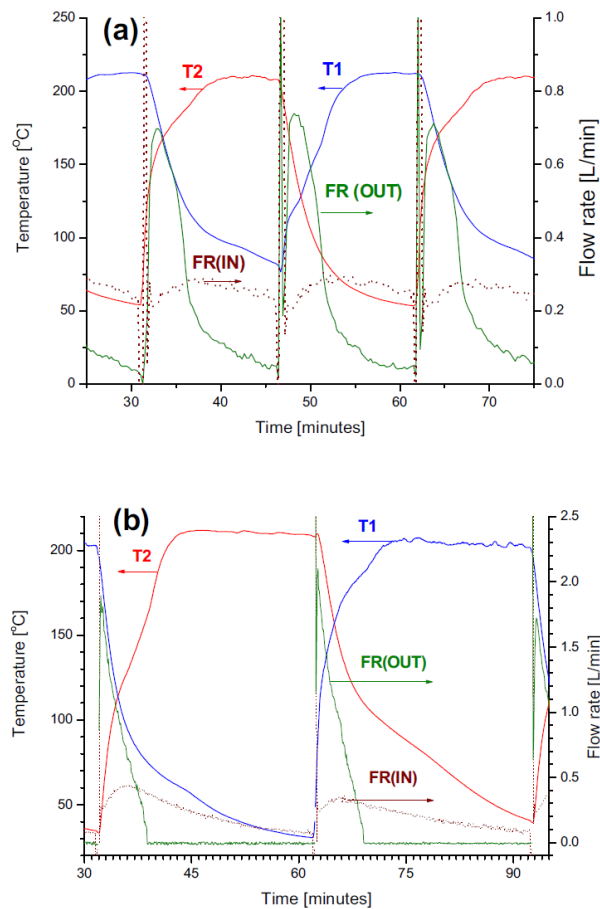

Fig. 6 – Operation cyclograms of the H_2 separation system.
Feed gas: H_2 (25%) + N_2 (balance); mixture input at
$P = 10$ bar; H_2 output at $P = 1$ bar; temperature set points:
$T_H = 200$ °C, $T_L = 20$ °C. Cycle duration and mixture flow
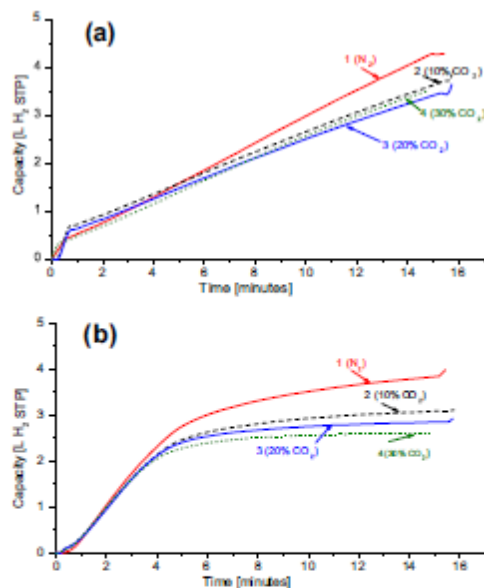rate: 15 min, 1.5 L/min (a); 30 min, 5 L/min (b).

14

Fig. 7 – Hydrogen absorption (a) and desorption (b) capacities of the MH separation reactor obtained during the operation of the H_2 separation system. Mixture input at $P = 10$ bar; H_2 output at $P = 1$ bar; temperature set points: $T_H = 200$ °C, $T_L = 20$ °C; cycle duration 15 min; mixture flow rate 1.5 L/min. Curve numbering corresponds to the following feed gas compositions: 1 – H_2 (25%) + N_2 (balance), 2–4 – H_2 (25%) + CO_2 (X%) + CO (100 ppm) + N_2 (balance), where X = 10, 20 and 30, respectively.
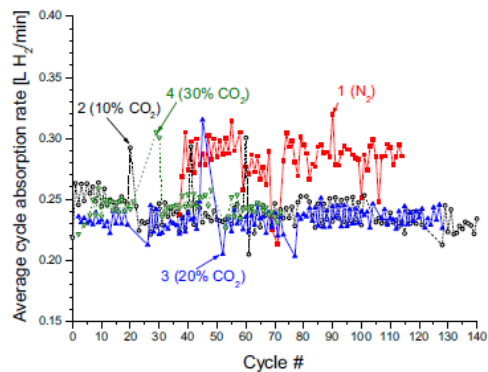

Fig. 8 – Average cycle H_2 absorption rate of the H_2 separation system for different compositions of the feed gas. The process parameters and feed gas compositions (corresponding to curve numbers) are the same as presented in Fig. 7. Deviations of the data from general trends are mainly caused by the variations of flow rate of feed gas (1…5 L/min).

It can be seen in Fig. 8 that the system exhibited stable performances in hydrogen absorption when operating in feedstock gases containing 25% of hydrogen, up to 30% of CO_2 and up to 100 ppm of CO. The introduction of CO_2 and CO into the feedstock gas resulted in ~20% decrease in the H_2 absorption capacity, as compared to that in the H_2 + N_2 mixture. However, no further decreases in H_2 absorption capacity were observed within 100e200 cycles without regeneration. The stability of the performances is credited to the improvement of poisoning tolerance of the MH material due to its F/Pd surface modification.

15

Table 3 summarises the results of mass-spectrometric gas analysis during the operation of the H_2 separation unit. Fig. 9 presents typical mass-spectra of the feeding gas of 25% H_2 + 20% CO_2 + 100 ppm CO + N_2 (A) and the separated hydrogen delivered during operation of the unit (B). As it can be seen, metal hydride hydrogen separation process exhibits the following features:

- Decrease of the concentration of the main impurities (N_2 and CO_2) in the output hydrogen. For N_2 (main peak at m/z = 28) the observed decrease is in 8-17 times (B/A = 0.06-0.12), and for CO_2-containing mixtures the CO_2 concentration (m/z = 44) decreases in 6e14 times (B/ A = 0.07-0.18). According to our calculations (see Table 4), it corresponds to the residual concentrations of N_2 and CO_2 not higher than 7.2 and 2.7%, respectively, and to the efficiencies of the removal of both components from 0.88 to 0.94.

Table 3 – Results of mass-spectrometric gas analysis during the operation of the H_2 separation unit.

m/z	Assumed components	Intensities [Torr] for different compositions of the feed gas											
		25% H_2 + N_2 (balance)			25% H_2 + 10% CO_2 + 100 ppm CO + N_2 (balance)			25% H_2 + 20% CO_2 + 100 ppm CO + N_2 (balance)			25% H_2 + 30% CO_2 + 100 ppm CO + N_2 (balance)		
		Feed gas (A)	Output H_2 (B)	B/A	Feed gas (A)	Output H_2 (B)	B/A	Feed gas (A)	Output H_2 (B)	B/A	Feed gas (A)	Output H_2 (B)	B/A
2	$(H_2)^+$	3.81E-06	2.10E-05	5.51	4.55E-06	1.75E-05	3.85	5.44E-06	1.80E-05	3.31	7.04E-06	2.42E-05	3.44
3	$(H_3)^+$	3.09E-09	1.41E-07	45.63	5.66E-09	1.03E-07	18.20	7.84E-09	1.04E-07	13.27	9.37E-09	1.34E-07	14.30
12	$(C)^+$				1.43E-09	3.08E-10	0.22	3.16E-09	2.73E-10	0.09	4.47E-09	2.10E-10	0.05
14	$(N)^+$, $(CH_2)^+$	2.08E-08	1.57E-09	0.08	1.65E-08	2.18E-09	0.13	1.38E-08	1.06E-09	0.08	1.08E-08	8.05E-10	0.07
15	$(CH_3)^+$				5.32E-10	1.97E-09	3.70	4.47E-10	2.48E-09	5.55	3.42E-10	2.65E-09	7.75
16	$(CH_4)^+$, $(O)^+$	3.28E-10	2.08E-10	0.63	4.13E-09	3.37E-09	0.82	7.82E-09	3.83E-09	0.49	1.13E-08	4.55E-09	0.40
17	$(OH)^+$	8.71E-10	1.23E-09	1.41	5.50E-10	1.27E-09	2.31	5.23E-10	1.51E-09	2.89	6.69E-10	1.95E-09	2.91
18	$(H_2O)^+$	3.57E-09	6.14E-09	1.72	1.88E-09	5.51E-09	2.93	1.54E-09	6.32E-09	4.10	1.95E-09	9.26E-09	4.75
22	$(CO_2)^{2+}$				4.17E-10	<1.00E-10	<0.24	8.57E-10	<1.00E-10	<0.12	1.19E-09	<1.00E-10	<0.08
28	$(N_2)^+$, $(CO)^+$	4.19E-07	3.56E-08	0.08	3.38E-07	3.97E-08	0.12	2.86E-07	1.58E-08	0.06	2.55E-07	1.56E-08	0.06
29	$(C_2H_5)^+$	4.47E-09	1.86E-09	0.42	4.57E-09	1.90E-09	0.42	4.21E-09	8.28E-10	0.20	3.72E-09	6.90E-10	0.19
32	$(O_2)^+$	5.02E-10	3.95E-10	0.79	1.80E-10	3.82E-10	2.12	2.03E-10	4.86E-10	2.39	<1.00E-10	2.14E-10	>2.14
44	$(CO_2)^+$	5.76E-10	4.28E-10	0.74	4.68E-08	8.64E-09	0.18	9.99E-08	6.93E-09	0.07	1.57E-07	1.17E-08	0.07
45	$(HCO_2)^+$				8.10E-10	3.48E-10	0.43	1.57E-09	2.76E-10	0.18	2.22E-09	2.84E-10	0.13
46	$(^{14}CO_2)^+$				1.97E-10	<1.00E-10	<0.51	3.25E-10	<1.00E-10	<0.31	3.85E-10	<1.00E-10	<0.26

• Significant increase of the intensities of hydrogen peaks. The intensity of main hydrogen peak (m/z = 2) increases in 3.3-5.5 times while for the peak m/z = 3 (H_3) the increase is in 13.3-45.6 times. The observed effect can be explained by the increase of H_2 concentration from ~25 to >90%, as well as by the higher ionisation efficiency of H_2 after its desorption from metal hydrides [35].
• 1.7-4.7 times increase of concentration of water vapours (m/z = 17, 18) in the output H_2, especially for CO_2-containing feed gases. The latter are also characterised by the reduction of O_2 concentration (m/z = 32) and a pronounced (4-8 times) increase of the peak with m/z = 15 which can be ascribed to $(CH_3)^+$ ion. This observation, together with the previously reported high chemical activity of H species generated from MH [36], allow us to assume that during H_2 separation process the H species interact with (i)

traces of oxygen in the feed gas to yield H_2O, and (ii) with CO_2 (and, most probably, CO) to yield $H_2O + CH_4$.

The main impurities detected in the output hydrogen were N_2 + CO (calculated concentrations up to 7%), CO_2 (up to 2.7%), water vapour (~0.5%) and light hydrocarbons (~0.3%). It can be concluded that the H_2 separation process exhibited high selectivity when the concentration of ballast and impurity gases in the feedstock (75% in total) was reduced to 5-8% in the output H_2 (see Table 4). Further removal of the impurities can be achieved by the introduction of the additional stage of hydrogen purification using MH materials that, at the optimal process management (e.g., blow-off of the first portions of the desorbed H_2), can result in the purity of the output hydrogen as high as ≥99.999% [14,19].
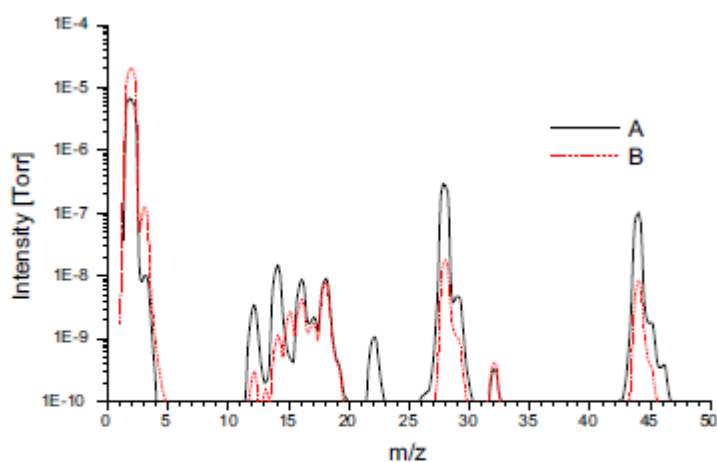

Fig. 9 – Mass spectra of the feed gas (A; 25% H_2 + 20% CO_2 + 100 ppm CO + N_2) and hydrogen separated during operation of the unit, B.

Table 4 – Performances of the H_2 separation unit according to results of mass-spectrometric analysis.

Feed gas	H$_2$ separation performances					
	Feed gas, C_0 [%]		Output H$_2$, $C_1 = C_0 \cdot B/A$ [%]		Efficiency, $(C_0 - C_1)/C_0$	
	N$_2$	CO$_2$	N$_2$	CO$_2$	N$_2$	CO$_2$
25% H$_2$ + N$_2$ (balance)	73.40	–	6.61	0	0.91	–
25% H$_2$ + 10% CO$_2$ + 100 ppm CO + N$_2$ (balance)	65.00	9.70	7.15	1.16	0.89	0.88
25% H$_2$ + 20% CO$_2$ + 100 ppm CO + N$_2$ (balance)	56.36	19.20	3.38	1.73	0.94	0.91
25% H$_2$ + 30% CO$_2$ + 100 ppm CO + N$_2$ (balance)	44.20	30.30	3.09	2.73	0.93	0.91

4. Conclusions

Further feasibility study of poisoning tolerance of surface modified hydride forming materials and their application for hydrogen separation from process gases containing carbon dioxide and monoxide has been carried out. Selection of suitable composition of the substrate has been done on the basis of analysis of PCT performances of several AB$_5$- type intermetallides, to provide maximum reversible hydrogen capacity at the process pressure-temperature conditions.

The selected La(Ni,Co,Mn,Al)$_5$ substrate alloy has been shown to be effectively surface-modified by fluorination followed by electroless deposition of palladium. The surface-modified material exhibited good coating quality, high cycle stability and minimal deterioration of kinetics of selective hydrogen absorption at room temperature, from gas mixtures containing 10% CO$_2$ and up to 100 ppm CO.

Integration of the surface-modified material into a prototype hydrogen separation system has shown feasibility of its application for hydrogen separation from feed gas containing H$_2$ at partial pressure of 2.5 bar, up to 30% CO$_2$ and up to 100 ppm CO. Despite of low process productivity caused by slow H$_2$ absorption due to mass transfer limitations in the gas phase, the hydrogen separation was characterised by stable performances throughout hundreds operation cycles, with a minor deterioration effect caused by the presence of CO$_2$ and CO. The H$_2$ separation process exhibited high selectivity when the concentration of ballast and impurity gases in the feed-stock (75% in total) was reduced to 5e8% in the output H$_2$. Further removal of the impurities can be achieved by the introduction of the additional stage of hydrogen purification using MH materials.

Acknowledgements

Appendix A. Supplementary data

Supplementary data related to this article can be found online at http://dx.doi.org/10.1016/j.ijhydene.2013.05.102.

References:

[1] Sandrock G. Applications of hydrides. In: Yurum Y, editor. Hydrogen energy system. Production and utilization of hydrogen and future aspects. NATO ASI Ser, Ser E, 295. Kluwer Acad Publ.; 1995. p. 253e80.

[2] Dantzer P. Properties of intermetallic compounds suitable for hydrogen storage applications. Mat Sci Eng 2002;A329e331:313e20.

[3] Sandrock G, Bowman Jr RC. Gas-based hydride applications: recent progress and future needs. J Alloys Compd 2003;356e357:794e9.

[4] Shmal'ko YuF, Solovei VV, Lotots'kyi MV, Klochko EV, Zavalii IYu, Ryabov OB, et al. Metal-hydride systems for processing hydrogen isotopes for power plants. Mat Sci 2001;37:689e706.

[5] Reilly JJ, Wiswall RH. Separation of hydrogen from other gases. Patent US 3793435; 1974.

[6] Billings RE. Hydrogen purification and storage system. Patent US 4108605; 1978.

[7] Ueno T, Isogai Y, Okawa T, Wakui N. Separating method for hydrogen from synthetic gas. Patent JP 55075903; 1980.

[8] Sheridan JJ, Eisenberg FG, Sandrock GD, Huston EL, Snape E, Stickles RP, et al. Recovering hydrogen from gas stream using metal hydride. Patent US 4360505; 1982.

[9] Sheridan JJ, Eisenberg FG, Greskovich EJ. Hydrogen separation from mixed gas streams using reversible metal hydrides. J Less-Common Met 1983;89:447e55.

[10] Goodell PD, Huston EL, Rudman PS, Sandrock GD. Methods of extracting hydrogen from a gas. Patent US 4687650; 1987.

[11] Peterson JC, DiMartino SP. Metal hydride adsorption process for hydrogen purification. Patent US 4696806; 1987.

[12] BogdanoricB. Method of separating and purifying hydrogen. Patents US 4695446; 1987, US 4749558; 1988.

[13] Zwart RL, Tinge JT. Continuous process for separating hydrogen in high purity from a gaseous hydrogen containing mixture. Patent US 5064627; 1991.

[14] Au M, Chen C, Ye Z, Fang T, Wu J, Wang O. The recovery, purification, storage and transport of hydrogen separated from industrial purge gas by means of mobile hydride containers. Int J Hydrogen Energy 1996;21:33e7.

[15] Monzyk BF, Tonkovich AY, Wang Y, VanderWiel DP, Perry ST, Fitzgerald SP, et al. Apparatus and methods for hydrogen separation/purification utilizing rapidly cycled thermal swing sorption. Patent US 6503298 B1; 2003.

[16] Suwarno S, Gosselin Y, Solberg JK, Maehlen JP, Williams M, Krogh B, et al. Selective hydrogen absorption from gaseous mixtures by BCC Ti-V alloys. Int J Hydrogen Energy 2012;37:4127e38.

[17] Miura S, Fujisawa A, Ishida M. A hydrogen purification and storage system using metal hydride. Int J Hydrogen Energy 2012;37:2794e9.

[18] Sandrock GD, Goodell PD. Cyclic life of metal hydrides with impure hydrogen: overview and engineering considerations. J Less-Common Met 1984;104:159e73.

[19] Tarasov BP, Shilkin SP. On the possibility to extract and to store high-purity hydrogen by hydrides of intermetallic compounds. Russ J Appl Chem 1995;68:21e6.

[20] Uchida H. Surface processes of H_2 on rare earth based hydrogen storage alloys with various surface modifications. Int J Hydrogen Energy 1999;24:861e9.

[21] Wang X-L, Iwata K, Suda S. Hydrogen purification using fluorinated $LaNi_{4.7}Al_{0.3}$ alloy. J Alloys Compd 1995;231:860e4.

[22] Bratanich TI, Bulanov VN, Skorokhod VV, Klimenko VP. Reversible hydriding of $LaNi_{5-x}Al_x$-Pd composites in the presence of carbon monoxide. Powder Metall Met Ceram 2000;39:575e83.

[23] Willey DB, Pederzolli D, Pratt AS, Swift J, Waltona A, Harris IR. Low temperature hydrogenation properties of platinum group metal treated, nickel metal hydride electrode alloy. J Alloys Compd 2002;330e332:806e9.

[24] Williams M, Lototsky MV, Linkov VM, Nechaev AN, Solberg JK, Yartys VA. Nanostructured surface coatings for the improvement of AB_5-type hydrogen storage intermetallics. Int J Energy Res 2009;33:1171e9.

[25] Williams M, Nechaev AN, Lototsky MV, Yartys VA, Solberg JK, Denys RV, et al. Influence of aminosilane surface functionalization of rare earth hydride-forming alloys on palladium treatment by electroless deposition and hydrogen sorption kinetics of composite materials. Mat Chem Phys 2009;115:136e41.

[26] Ren J, Williams M, Lototskyy M, Davids W, Ulleberg Ø. Improved tolerance of Pd/Cu-treated metal hydride alloys towards air impurities. Int J Hydrogen Energy 2010;35:8626e30.

[27] Williams M, Lototsky M, Nechaev A, Yartys V, Solberg JK, Denys RV, et al. Palladium mixed-metal surface-modified AB_5-type intermetallides enhance hydrogen sorption kinetics. S Afr J Sci 2010;106(9/10):6. http://dx.doi.org/10.4102/sajs.v106i9/10.310. Art. #310.

[28] Lototsky MV, Williams M, Yartys VA, Klochko YeV, Linkov VM. Surface-modified advanced hydrogen storage alloys for hydrogen separation and purification. J Alloys Compd 2011;509(Suppl. 2):S555e61.

[29] Williams M, Lototskyy MV, Nechaev AN, Linkov VM. Method of surface modification of metallic hydride forming materials. Patent US 8354552 B2; applications ZA 2007/09455,WO 2009/066263 A1.

[30] Williams M, Lototskyy MV, Nechaev AN, Linkov VM. Hydride forming material. Patent ZA 2008/09123.

[31] Lototskyy M, Williams M, Klochko Ye, Modibane KD, Linkov V. Hydrogen separation from CO_2- and CO-containing gases using surface-modified metal hydrides. In: World Congress on Engineering and Technology (CET2011), Shanghai/China, Oct. 28e30, 2011(Paper ID 24247). Proceedings of 2011 World Congress on Engineering and Technology, 03. IEEE Press; 2011. 446e451 (0521-1914361).

[32] Lototskyy M, Modibane KD, Williams M, Klochko Ye, Linkov V, Pollet BG. Application of surface-modified metal hydrides for hydrogen separation from gas mixtures containing carbon dioxide and monoxide. J Alloys Compd 2013. http://dx.doi.org/10.1016/j.jallcom.2013.02.096.

[33] Lototsky MV, Yartys VA, Marinin VS, Lototsky NM. Modelling of phase equilibria in metalehydrogen systems. J Alloys Compd 2003;356e357:27e31.

[34] Dunikov D, Borzenko V, Malyshenko S. Influenc of impurities on hydrogen absorption in a metal hydride reactor. Int J Hydrogen Energy 2012;37:13843e8.

[35] Shmal'ko YuF, Klochko YeV, Lototsky MV. Influence of isotopic effect on the shift of the ionization potentials of hydrogen desorbed from the metal hydride surface. Int J Hydrogen Energy 1996;21:1057e9.

[36] Shmal'ko YuF, Lototsky MV, Klochko YeV, Solovey VV. The formation of excited H species using metal hydrides. J Alloys Compd 1995;231:856e9.